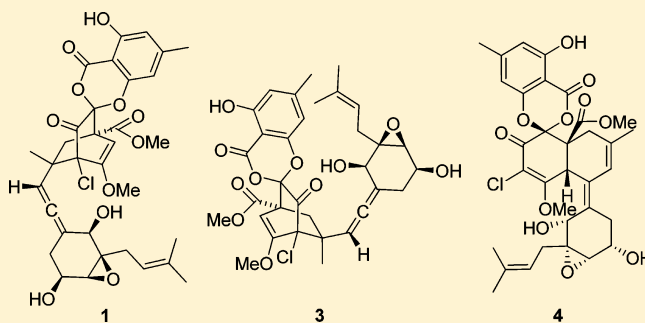


Spiroketal of *Pestalotiopsis fici* Provide Evidence for a Biosynthetic Hypothesis Involving Diversified Diels–Alder Reaction CascadesLing Liu,<sup>†</sup> Yan Li,<sup>‡</sup> Li Li,<sup>§</sup> Ya Cao,<sup>\*,⊥</sup> Liangdong Guo,<sup>†</sup> Gang Liu,<sup>†</sup> and Yongsheng Che<sup>\*,‡</sup><sup>†</sup>State Key Laboratory of Mycology, Institute of Microbiology, Chinese Academy of Sciences, Beijing 100190, People's Republic of China<sup>‡</sup>Beijing Institute of Pharmacology & Toxicology, Beijing 100850, People's Republic of China<sup>§</sup>Institute of Materia Medica, Chinese Academy of Medical Sciences & Peking Union Medical College, Beijing 100050, People's Republic of China<sup>⊥</sup>Cancer Research Institute, Xiangya School of Medicine, Central South University, Changsha, Hunan 410078, People's Republic of China

## S Supporting Information

**ABSTRACT:** Chloropestolides B–G (1–6), six new metabolites featuring the chlorinated spiro[benzo[*d*][1,3]dioxine-2,7'-bicyclo[2.2.2]octane]-4,8'-dione (1–3) and spiro[benzo[*d*][1,3]dioxine-2,1'-naphthalene]-2',4-dione (4–6) skeletons, and their putative biosynthetic precursor dechloromaldoxin (7) were isolated from the scale-up fermentation cultures of the plant endophytic fungus *Pestalotiopsis fici*. The structures of 1–7 were determined mainly by NMR experiments. The absolute configurations of 1–3 were deduced by analogy to the previously isolated metabolites from the same fungus (9 and 13–18), whereas those of 4, 5, and 7 were assigned by electronic circular dichroism (ECD) calculations. Structurally, the spiroketal skeletons found in 1–3 and 4–6 could be derived from 2,6-dihydroxy-4-methylbenzoic acid with chlorinated bicyclo[2.2.2]oct-2-en-5-one and 4a,5,8,8a-tetrahydronaphthalen-2(1*H*)-one, respectively. Biogenetically, compounds 1–6 were derived from the same Diels–Alder precursors as the previously isolated 9 and 12–18. In addition, compounds 2 and 3 were proposed as the biosynthetic intermediates of 17 and 16, respectively. Compound 1 was cytotoxic to three human tumor cell lines.



## ■ INTRODUCTION

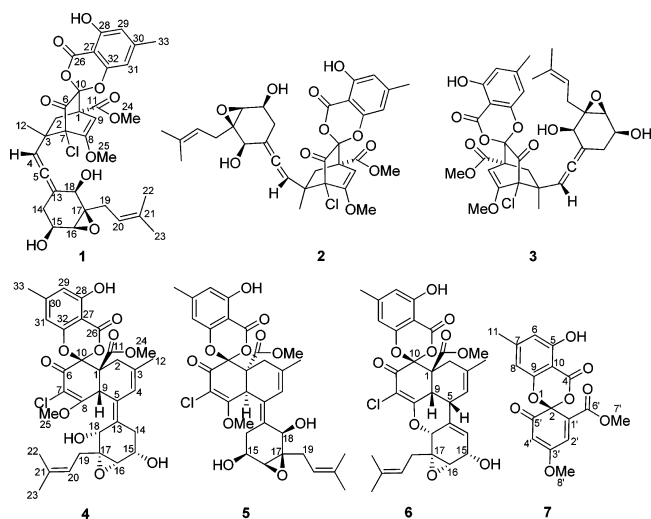
Endophytic fungi inhabiting the normal tissues of host plants are well-known producers of bioactive natural products.<sup>1–4</sup> The species of the *Pestalotiopsis* genus have attracted much attention due to the discovery of structurally diverse and biologically active secondary metabolites.<sup>5</sup> Our chemical studies of this genus also afforded a variety of bioactive compounds.<sup>6</sup> During the course of the investigations, a strain of *P. fici* (W106-1), isolated from the branches of *Camellia sinensis* (Theaceae) in a suburb of Hangzhou, People's Republic of China, was grown in different solid–substrate fermentation cultures.<sup>7–10</sup> Fractionation of the resulting crude extracts afforded unique natural products, including chloropupukeananin (9; Scheme 1), the first chlorinated tricyclo[4.3.1.0<sup>3,7</sup>]decane (pupukeanane) skeleton, and its putative biosynthetic precursors, pestheic acid (10; Scheme 1) and iso-A82775C (11; Scheme 1).<sup>7</sup> Subsequent studies of the same extracts led to the isolation of additional seven novel metabolites, named chloropestolide A (12; Scheme 1),<sup>11</sup> chloropupukeanolides A and B and chloropupukeanone A (13–15; Scheme 1),<sup>12</sup> and chloropupukeanolides C–E (16–18; Scheme 1),<sup>13</sup> originating from the same Diels–Alder

precursors as 9. Recently, the Kobayashi group proposed that the putative biosynthetic precursor 10 was first oxidized to maldoxin (10a),<sup>14</sup> which possesses a reactive diene known as masked O-benzoquinone,<sup>15</sup> and then subjected to a reverse electron demand Diels–Alder (REDDA) reaction<sup>16</sup> with the terminal alkene in 11 to form the core structure of this class of metabolites.<sup>17</sup> Specifically, reaction of the diene from the ether face (the side of the ether oxygen attached to the ketal carbon) of 10a with the allene in 11 afforded 12 and 16 as the *endo* and *exo* REDDA cycloadducts, respectively, whereas compounds 9, 13–15, 17, and 18 were the *exo* REDDA products resulting from reaction of the diene from the carboxylate face (the side of the carboxyl group attached to the ketal carbon) of 10a with the allene in 11 (Scheme 1). Subsequently, the Snider group synthesized 10a from chloroisosulochrin via 10 using a biomimetic route to explore facial selectivity for the Diels–Alder reaction of 10a with an isopropenylallene,<sup>18,19</sup> and the major products were found to be the *endo* and *exo* REDDA

Received: December 29, 2012

adducts reacting from the carboxylate face of **10a** with **11**.<sup>19</sup> In addition, the normal electron demand Diels–Alder (NEDDA)<sup>16</sup> adducts in which **10a** reacted as a dienophile and **11** as a diene were also obtained.<sup>19</sup>

To better understand the naturally occurring Diels–Alder reactions leading to the formation of these novel metabolites and provide useful information for synthetic chemists in their future endeavors to synthesize related natural products, the EtOAc extract prepared from a scale-up fermentation were separated exhaustively. Six new Diels–Alder cycloadducts from **10a** and **11** were obtained, including three REDDA and three NEDDA products, which we named chloropestolides B–D (**1**–**3**) and chloropestolides E–G (**4**–**6**), respectively. In addition, dechloromaldoxin (**7**), a new congener of maldoxin (**10a**), was also isolated from the same extract. Details of the isolation, structure elucidation, cytotoxicity, and plausible biogenesis of **1**–**7** are reported herein.



## RESULTS AND DISCUSSION

The fungus *P. fici* was re fermented on rice (3 kg) for 40 days and extracted repeatedly with EtOAc. The resulting crude extract was fractionated by silica gel vacuum liquid chromatography (VLC), followed by Sephadex LH-20 column chromatography and reversed-phase (RP) HPLC to afford the new metabolites chloropestolides B–G (**1**–**6**) and dechloromaldoxin (**7**).

The molecular formula of chloropestolide B (**1**) was determined to be  $C_{33}H_{35}ClO_{11}$  (16 degrees of unsaturation) by HRESIMS. Analysis of the NMR data of **1** (Table 1) revealed the presence of three exchangeable protons ( $\delta_H$  3.94, 4.17, and 9.80, respectively), six methyl groups including two methoxys, three methylenes, three oxymethines, 13  $sp^2$  carbons including five methines, five  $sp^3$  quaternary carbons including three bonded to heteroatoms, two carboxylic carbons ( $\delta_C$  163.1 and 169.4, respectively), and one ketone carbon ( $\delta_C$  191.5). These data revealed structural similarity to chloropestolide A (**12**).<sup>11</sup> Analysis of the  $^1H$ – $^1H$  COSY and HMBC data of **1** defined the same 5-hydroxy-7-methyl-4*H*-benzo[*d*][1,3]dioxin-4-one and isoprenylated 2,3-epoxyvinylidenecyclohexan-1,4-diol moieties as found in **12**. Further interpretation of the 2D NMR data established a polysubstituted bicyclo[2.2.2]oct-2-en-5-one unit joined to the benzo[*d*][1,3]dioxin-4-one through a spiro carbon at C-10 and linked to the isoprenylated 2,3-

**Table 1.** NMR Data for **1** (Acetone- $d_6$ )

position	$\delta_C^a$	$\delta_H^b$ , mult (J, Hz)	HMBC <sup>a</sup>	NOESY <sup>c</sup>
1	51.6, qC		1, 3, 4, 7, 9, 10, 11, 12	
2a	40.0, CH <sub>2</sub>	2.28, d (13)	1, 3, 4, 7, 9, 10, 11, 12	4, 9
2b		2.56, d (13)		12
3	44.9, qC		2, 5, 12, 13, 14, 18	
4	97.3, CH	5.18, d (3.5)		2a, 12
5	203.1, qC			
6	191.5, qC			
7	81.7, qC			
8	151.2, qC		1, 2, 7, 8, 10, 11	
9	97.0, CH	5.62, s		2a
10	98.4, qC			
11	169.4, qC		2, 3, 4, 7	
12	24.0, CH <sub>3</sub>	1.21, s		2b, 4
13	105.9, qC		5, 13, 15, 16, 18	
14a	31.2, CH <sub>2</sub>	2.15, dd (16, 5.5)	5, 13, 15, 16, 18	
14b		2.35, ddd (16, 10, 3.5)		
15	68.5, CH	3.98, ddd (10, 7.0, 5.5)	14, 15, 17, 18, 19	
16	63.2, CH	3.25, br s		19, 20
17	65.6, qC		5, 13, 14, 16, 19	
18	68.7, CH	4.21, d (9.0)	16, 17, 18, 20, 21	19, 20
19a	33.5, CH <sub>2</sub>	2.09, dd (16, 7.0)	16, 17, 18, 20, 21	16, 18
19b		2.81, dd (16, 7.0)	17, 19, 22, 23	16, 18
20	119.3, CH	5.16, t (7.0)		16, 18
21	135.6, qC		20, 21, 23	
22	18.1, CH <sub>3</sub>	1.65, s	20, 21, 22	
23	26.0, CH <sub>3</sub>	1.75, s	11	
24	53.4, CH <sub>3</sub>	3.75, s	8	
25	57.1, CH <sub>3</sub>	3.78, s		
26	163.1, qC			
27	96.8, qC			
28	161.5, qC		26, 27, 28, 31, 33	
29	112.6, CH	6.52, s		
30	151.8, qC		26, 27, 29, 32, 33	
31	108.3, CH	6.30, s		
32	155.8, qC		29, 30, 31	
33	22.3, CH <sub>3</sub>	2.30, s	14, 16	
OH-15		4.17, d (7.0)	17, 18	
OH-18		3.94, d (9.0)	27, 28, 29	
OH-28		9.80, s		

<sup>a</sup>Recorded at 125 MHz. <sup>b</sup>Recorded at 500 MHz. <sup>c</sup>Recorded at 500 MHz.

epoxyvinylidenecyclohexan-1,4-diol at C-3. These data permitted assignment of the planar structure of **1**, which is the same as that of **12**.

The epoxyvinylidenecyclohexanediol in **1** was assigned the same relative configuration as in **9** and **12**–**18** by comparison of the  $^1H$ – $^1H$  coupling constants and NOESY data.<sup>7,11–13</sup> NOESY correlations (Figure 1) of H-2a with H-4 and H-9 and of H<sub>3</sub>-12 with H-2b and H-4 indicated that C-1, C-3, and C-7 in **1** adopt the same relative configurations as in **12**, which were secured by X-ray crystallography.<sup>11</sup> Since compounds **1** and **12** are both the *endo* REDDA adducts of **10a** and **11** (Scheme 1), the absolute configuration of C-10 in **1** was deduced to be the same as that in **12** on the basis of biosynthetic considerations. A

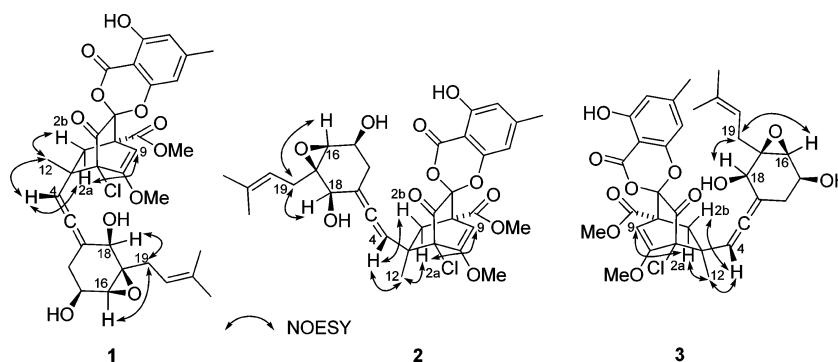


Figure 1. Key NOESY correlations for 1–3.

Table 2. NMR Data for 2 and 3 (Acetone- $d_6$ )

position	2			3		
	$\delta_C^a$	$\delta_H^b$ mult (J, Hz)	HMBC <sup>a</sup>	$\delta_C^c$	$\delta_H^d$ mult (J, Hz)	HMBC <sup>c</sup>
1	51.8, qC			51.5, qC		
2a	39.6, CH <sub>2</sub>	1.92, d (14)	1, 3, 4, 7, 9, 10, 11, 12	42.7, CH <sub>2</sub>	2.06, d (14)	1, 3, 4, 7, 9, 10, 11, 12
2b		2.89, d (14)	1, 3, 4, 7, 9, 10, 11, 12		2.95, d (14)	1, 3, 4, 7, 9, 10, 11, 12
3	45.6, qC			44.9, qC		
4	95.5, CH	5.18, d (3.0)	2, 5, 12, 13, 14, 18	96.2, CH	5.21, d (3.5)	2, 12, 13
5	202.9, qC			203.7, qC		
6	191.2, qC			190.0, qC		
7	81.5, qC			81.6, qC		
8	151.3, qC			151.0, qC		
9	97.4, CH	5.71, s	1, 2, 7, 8, 10, 11	98.0, CH	5.66, s	1, 2, 7, 8, 10, 11
10	98.2, qC			97.3, qC		
11	169.4, qC			169.1, qC		
12	26.3, CH <sub>3</sub>	1.17, s	2, 3, 4, 7	25.8, CH <sub>3</sub>	1.17, s	2, 3, 4, 7
13	105.6, qC			105.0, qC		
14a	30.3, CH <sub>2</sub>	2.27, dd (16, 5.5)	5, 13, 15, 16, 18	30.7, CH <sub>2</sub>	2.11, dd (16, 5.5)	5, 13, 15, 16, 18
14b		2.32, ddd (16, 10, 3.0)	5, 13, 15, 16, 18		2.25, ddd (16, 10, 3.5)	5, 13, 15, 16, 18
15	68.5, CH	4.13, ddd (10, 6.0, 5.5)		68.0, CH	4.01, ddd (10, 6.0, 5.5)	
16	63.3, CH	3.24, br s	14, 15, 17, 18, 19	63.5, CH	3.24, br s	14, 15, 17, 18, 19
17	65.7, qC			65.8, qC		
18	68.5, CH	4.26, d (8.5)	5, 13, 14, 19	68.2, CH	4.32, d (9.0)	5, 13, 14
19a	33.7, CH <sub>2</sub>	2.00, dd (15, 6.0)	16, 17, 18, 20, 21	33.5, CH <sub>2</sub>	2.04, dd (16, 7.0)	16, 17, 18, 20, 21
19b		2.78, dd (15, 6.0)	16, 17, 18, 20, 21		2.78, dd (16, 7.0)	16, 17, 18, 20, 21
20	119.3, CH	5.13, t (6.0)	22, 23	119.2, CH	5.14, t (7.0)	19, 22, 23
21	135.6, qC			135.6, qC		
22	18.0, CH <sub>3</sub>	1.63, s	20, 21, 23	18.0, CH <sub>3</sub>	1.63, s	20, 21, 23
23	26.0, CH <sub>3</sub>	1.69, s	20, 21, 22	25.9, CH <sub>3</sub>	1.68, s	20, 21, 22
24	53.4, CH <sub>3</sub>	3.72, s	11	53.4, CH <sub>3</sub>	3.77, s	11
25	57.2, CH <sub>3</sub>	3.81, s	8	57.2, CH <sub>3</sub>	3.80, s	8
26	163.2, qC			163.8, qC		
27	96.8, qC			96.4, qC		
28	161.4, qC			161.4, qC		
29	112.6, CH	6.51, s	27, 28, 31, 33	113.0, CH	6.55, s	27, 28, 31, 33
30	151.8, qC			151.8, qC		
31	108.3, CH	6.30, s	26, 27, 29, 32, 33	108.5, CH	6.57, s	26, 27, 29, 32, 33
32	155.8, qC			154.4, qC		
33	22.3, CH <sub>3</sub>	2.29, s	29, 30, 31	22.3, CH <sub>3</sub>	2.32, s	29, 30, 31
OH-15		3.99, d (6.0)	14, 15, 16		4.14, d (6.0)	14, 16
OH-18		3.87, d (8.5)	13, 17, 18		3.89, d (9.0)	17, 18
OH-28		9.78, br s	27, 28, 29		9.80, br s	

<sup>a</sup>Recorded at 125 MHz. <sup>b</sup>Recorded at 500 MHz. <sup>c</sup>Recorded at 150 MHz. <sup>d</sup>Recorded at 600 MHz.

NOESY correlation of H<sub>3</sub>-12 with H-31 in **12** revealed the proximity of H<sub>3</sub>-12 to the ether oxygen of the spiroketal, indicating that **12** is indeed an *endo* REDDA adduct, whereas

the lack of a NOESY correlation between H<sub>3</sub>-12 and H-31 in **1** implied that H<sub>3</sub>-12 was close to the carboxylate oxygen of the spiroketal, suggesting that **1** was also an *endo* REDDA

Table 3. NMR Data for 4–6 (Acetone- $d_6$ )

position	4			5			6		
	$\delta_C^a$	$\delta_H^b$ mult (J, Hz)	HMBC <sup>a</sup>	$\delta_C^a$	$\delta_H^b$ mult (J, Hz)		$\delta_C^a$	$\delta_H^b$ mult (J, Hz)	
1	54.9, qC			55.0, qC			54.2, qC		
2a	31.5, CH <sub>2</sub>	2.24, d (19)	1, 3, 4, 10, 11	31.1, CH <sub>2</sub>	2.24, d (19)		30.2, CH <sub>2</sub>	2.11, d (19)	
2b		2.98, d (19)	1, 3, 4, 9, 11, 12		3.02, d (19)			2.92, d (19)	
3	135.7, qC			134.9, qC			131.6, qC		
4	122.0, CH	6.40, s	2, 5, 9, 12, 13	121.7, CH	6.52, s		125.7, CH	5.32, br s	
5	126.7, qC			126.1, qC			34.0, CH	3.56, br s	
6	181.7, qC			181.8, qC			180.3, qC		
7	109.2, qC			110.2, qC			106.2, qC		
8	174.6, qC			173.7, qC			173.0, qC		
9	42.2, CH	5.11, s	1, 2, 4, 5, 6, 7, 8, 10, 11, 13	41.4, CH	4.87, s		36.0, CH	4.47, d (6.5)	
10	102.9, qC			102.9, qC			103.4, qC		
11	168.7, qC			168.7, qC			168.9, qC		
12	23.4, CH <sub>3</sub>	1.82, s	2, 3, 4	23.5, CH <sub>3</sub>	1.83, s		22.9, CH <sub>3</sub>	1.68, s	
13	136.6, qC			137.5, qC			131.3, qC		
14a	28.9, CH <sub>2</sub>	2.29, dd (13, 11)	5, 13, 15, 16	29.9, CH <sub>2</sub>	2.39, dd (13, 11)		126.8, CH	5.64, t (2.0)	
14b		2.65, dd (13, 4.5)	5, 13, 15, 16, 18		2.65, dd (13, 4.5)				
15	69.1, CH	3.63, ddd (11, 5.5, 4.5)	16	68.3, CH	3.93, ddd (11, 5.5, 4.5)		65.9, CH	4.55, dd (6.5, 2.0)	
16	63.4, CH	3.26, s	14, 15, 17, 19	62.9, CH	3.23, s		59.2, CH	3.41, s	
17	65.5, qC			65.0, qC			59.6, qC		
18	65.8, CH	4.82, d (9.0)	5, 13, 14, 19	65.3, CH	4.59, d (10)		76.9, CH	5.35, s	
19a	33.9, CH <sub>2</sub>	2.17, dd (15, 6.5)	16, 17, 20, 21	33.5, CH <sub>2</sub>	2.17, dd (14, 7.5)		31.1, CH <sub>2</sub>	2.33, dd (14, 7.5)	
19b		2.88, dd (15, 6.5)	16, 17, 20, 21		2.88, dd (14, 7.5)			2.97, dd (14, 7.5)	
20	119.4, CH	5.29, t (6.5)	19, 22, 23	119.2, CH	5.07, t (7.5)		118.2, CH	5.20, t (7.5)	
21	135.8, qC			135.4, qC			136.7, qC		
22	26.1, CH <sub>3</sub>	1.74, s	20, 21, 23	25.9, CH <sub>3</sub>	1.72, s		17.9, CH <sub>3</sub>	1.67, s	
23	18.3, CH <sub>3</sub>	1.78, s	20, 21, 22	18.0, CH <sub>3</sub>	1.70, s		26.0, CH <sub>3</sub>	1.72, s	
24	53.4, CH <sub>3</sub>	3.66, s	11	53.5, CH <sub>3</sub>	3.61, s		53.9, CH <sub>3</sub>	3.79, s	
25	63.3, CH <sub>3</sub>	4.16, s	8	63.1, CH <sub>3</sub>	4.13, s				
26	164.4, qC			162.7, qC			164.4, qC		
27	98.7, qC			97.0, qC			98.7, qC		
28	161.1, qC			161.7, qC			161.0, qC		
29	113.0, CH	6.52, s	27, 28, 31, 33	112.0, CH	6.49, s		113.0, CH	6.49, s	
30	151.1, qC			152.3, qC			151.0, qC		
31	108.2, CH	6.43, s	26, 27, 29, 32, 33	108.0, CH	6.49, s		107.9, CH	6.27, s	
32	153.9, qC			157.5, qC			154.0, qC		
33	22.2, CH <sub>3</sub>	2.27, s	29, 30, 31	22.4, CH <sub>3</sub>	2.35, s		22.2, CH <sub>3</sub>	2.27, s	
OH-15		4.18, d (5.5)	14, 15, 16		4.30, d (5.5)			4.41, d (6.5)	
OH-18		3.52, d (9.0)	18		3.83, d (10)				
OH-28		9.86, s	27, 28, 29		9.74, s			9.81, s	

<sup>a</sup>Recorded at 150 MHz. <sup>b</sup>Recorded at 600 MHz.

cycloadduct. Collectively, compound **1** was deduced to have the 1S,3S,5aS,7R,10R,15S,16S,17R,18R absolute configuration.

Chloropestolide C (**2**) was obtained as a mixture with **17** in a ratio of 25:1, which slowly changed to 20:1 over a period of 72 h, as determined by integration of some well-resolved <sup>1</sup>H NMR resonances (e.g., H-4 and H-9; Figure S4 (Supporting Information)) for each compound. Efforts to obtain pure **2** were unsuccessful due to repeated cyclization from **2** to **17**. Therefore, the structure elucidation of **2** was performed on the mixture. HRESIMS analysis of **2** gave the same elemental composition, C<sub>33</sub>H<sub>35</sub>ClO<sub>11</sub>, as **1**. The <sup>1</sup>H and <sup>13</sup>C NMR spectra of **2** showed resonances similar to those of **1**, except that the resonances for C-2, C-4, and C-12 were slightly different. Interpretation of the <sup>1</sup>H–<sup>1</sup>H COSY and HMBC data for **2** established the same gross structure as **1** and **12**, indicating that **2** was a stereoisomer of **1** and **12**.

The epoxyvinylidenecyclohexanediol moiety in **2** was also assigned the same relative configuration as in **1**, **9**, and **12**–**18**

by comparison of the <sup>1</sup>H–<sup>1</sup>H coupling constants and NOESY data for relevant protons (Figure 1).<sup>7,11–13</sup> NOESY correlations of H-2a with H-9 and H<sub>3</sub>-12 and of H-4 with H-2b and H<sub>3</sub>-12 defined the relative configurations for C-1, C-3, and C-7, indicating that **2** is an *exo* REDDA adduct of **10a** and **11** (Scheme 1). The relative configuration of C-10 was deduced to be the same as that in **17** due to the aforementioned cyclization from **2** to **17**. Since the absolute configuration of **17**, the cyclization product of **2**, was already assigned by quantum chemical CD calculations,<sup>13</sup> the absolute configuration of **2** was proposed to be 1S,3R,5aS,7R,10R,15S,16S,17R,18R.

Chloropestolide D (**3**) was also isolated as a mixture with **16** in a ratio of 9:1 which gradually changed to 5:1 over 120 h (Figure S7 (Supporting Information)). Its structure determination was also performed on the mixture due to repeated cyclization from **3** to **16**. Compound **3** was assigned the same molecular formula, C<sub>33</sub>H<sub>35</sub>ClO<sub>11</sub>, as **1** and **2** on the basis of HRESIMS analysis. Interpretation of its <sup>1</sup>H and <sup>13</sup>C NMR data



(Table 2) revealed the same planar structure as **1** and **2**, suggesting that **3** is a stereoisomer of **1** and **2**. The epoxyvinylidenecyclohexanediol and C-10 in **3** were deduced to have the same relative configurations as in **1**, **2**, **9**, and **12**–**18** based on biosynthetic considerations, and were supported by NOESY data (Figure 1). NOESY correlations of H-2a with H-9 and H<sub>3</sub>-12, and of H-4 with H-2b and H<sub>3</sub>-12 were found in **2** and **3** (Figure 1), suggesting the same relative configurations for C-1, C-3, and C-7 for both compounds. Since the absolute configuration of **16** was already established by X-ray crystallography,<sup>13</sup> the cyclization precursor **3** was deduced to have the 1R,3S,5aS,7S,10R,15S,16S,17R,18R absolute configuration.

Chloropestolide E (**4**) was assigned the same molecular formula, C<sub>33</sub>H<sub>35</sub>ClO<sub>11</sub> (16 degrees of unsaturation), as **1**–**3** by HRESIMS. Its <sup>1</sup>H and <sup>13</sup>C NMR spectra showed resonances for three exchangeable protons ( $\delta_{\text{H}}$  3.52, 4.18, and 9.86), six methyl groups including two O-methyls, three methylenes, three oxymethines, 15 sp<sup>2</sup> carbons including five methines, three sp<sup>3</sup> quaternary carbons including two heteroatom-bonded, two carboxylic carbons ( $\delta_{\text{C}}$  164.4 and 168.7, respectively), and one ketone carbon ( $\delta_{\text{C}}$  181.7). These data accounted for all the NMR resonances except for one chlorine atom. Analysis of its NMR data (Table 3) revealed the presence of the same 5-hydroxy-7-methyl-4H-benzo[d][1,3]dioxin-4-one moiety as found in **1**–**3**, but the remaining portion was significantly different, warranting detailed 2D NMR analysis. Interpretation of the HMBC data of **4** established the same C-17 isoprenylated 2,3-epoxycyclohexane-1,4-diol as that appearing in **1**–**3**. HMBC correlations from H<sub>2</sub>-2 to C-3, C-4, and C-12 and from H<sub>3</sub>-12 to C-2, C-3, and C-4 connected both C-2 and C-12 to the C-3/C-4 olefin at C-3. Cross-peaks from H-4 to C-5, C-9, and C-13, from H-9 to C-4, C-5, and C-13, and from H<sub>2</sub>-14 and H-18 to C-5 located C-4 and C-9 at the allylic positions of the C-5/C-13 olefin. Correlations from H<sub>2</sub>-2 and H-9 to the C-1 quaternary carbon, C-10 ketal carbon, and C-11 carboxylic carbon indicated that C-1 is attached to C-2, C-9, C-10, and C-11, completing the cyclohexene unit in **4**. HMBC cross peaks from H-9 to the C-7 and C-8 olefinic carbons, plus the chemical shift for C-6 ( $\delta_{\text{C}}$  181.7), indicated that the C-7/C-8 olefin is connected to C-9 and C-6 at C-8 and C-7, respectively, and the latter was supported by a four-bond HMBC correlation of H-9 with C-6.<sup>20</sup> In turn, correlations from H<sub>3</sub>-24 to C-11 and from H<sub>3</sub>-25 to C-8 located the two methoxys at C-11 and C-8, respectively. Considering the chemical shift of C-7 ( $\delta_{\text{C}}$  109.2) and the hexacyclic nature of **4**, the chlorine atom was attached to C-7, and C-6 was linked to C-10 by default to complete the 3-chloro-4a,5,8,8a-tetrahydronaphthalen-2(1H)-one unit joined to the benzo[d][1,3]-dioxin-4-one through a spiro carbon at C-10. On the basis of these data, the planar structure of **4** is proposed as shown.

The absolute configuration of the epoxycyclohexanediol in **4** was deduced to be the same as in **1**–**3** on the basis of biosynthetic considerations and by comparison of the <sup>1</sup>H–<sup>1</sup>H coupling constants and NOESY data for relevant protons (Figure 2). A NOESY correlation of H-9 with H-18 revealed their proximity in space, and that of H-4 with H-14b defined the *Z* geometry for the C-5/C-13 olefin. The absolute configuration of C-1, C-9, and C-10 in **4** was deduced by comparison of the experimental and simulated ECD spectra generated by time-dependent density functional theory (TDDFT).<sup>21</sup> Since the epoxycyclohexane-1,4-diol is insignificant to the CD properties of **4**, a simplified structure (**8**; Figure

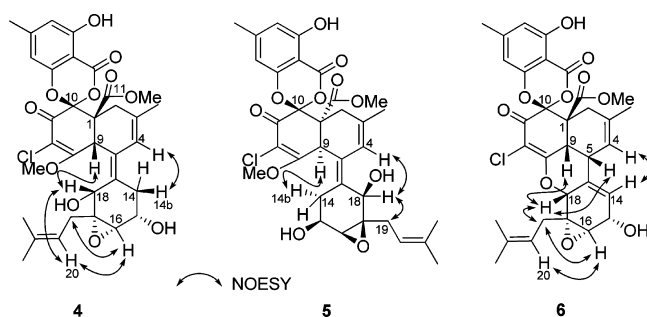


Figure 2. Key NOESY correlations for **4**–**6**.

**3**) was used for ECD calculations. Considering the fact that **4** was derived from **10a** and **11** via a Diels–Alder reaction

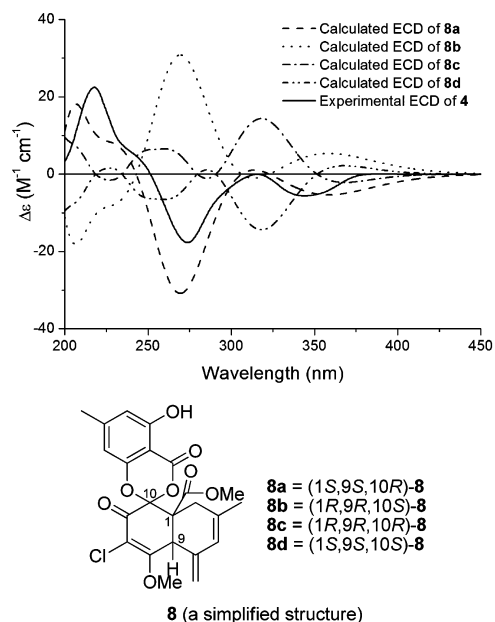
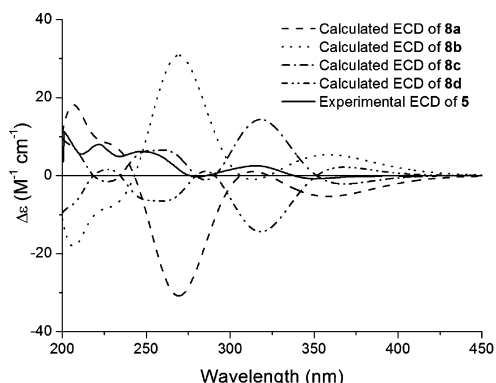


Figure 3. Experimental CD spectrum of **4** in MeOH and the calculated ECD spectra of **8a**–**d**. Structures **8a**–**d** represent four possible stereoisomers of **8**.

(Scheme 1), H-9 and COOCH<sub>3</sub> should be on the same face of the ring system.<sup>15,19,22</sup> Therefore, only the (1S,9S,10R)-**8**, (1R,9R,10S)-**8**, (1R,9R,10R)-**8**, and (1S,9S,10S)-**8** (**8a**–**d**; Figure 3) configurations were calculated. A systematic conformational analysis was performed for **8a**–**d** via the molecular operating environment (MOE) software package using the MMFF94 molecular mechanics force field calculation. The MMFF94 conformational search followed by reoptimization using TDDFT at the B3LYP/6-31G(d) basis set level afforded four lowest-energy conformers each for **8a/8b** and **8c/8d**, respectively (Figures S17 and S18 (Supporting Information)). The overall calculated ECD spectra of **8a,b** were then generated by Boltzmann weighting of their lowest-energy conformers with 52.1, 28.8, 9.5, and 9.6% populations, respectively, by their relative free energies. In a similar fashion, the overall calculated ECD spectra of **8c,d** were also generated. The absolute configuration of **4** was then extrapolated by comparison of the experimental and calculated ECD spectra of **8a**–**d**. The overall pattern of the experimental CD spectrum of **4** matches the calculated ECD curve of **8a**, with two negative Cotton effects (CEs) in the region of 260–400 nm and a

positive effect at 200–250 nm (Figure 3). Therefore, the absolute configuration of **4** was deduced to be 1*S*,9*S*,10*R*,15*S*,16*S*,17*R*,18*R*.

Chloropestolide F (**5**) had the same molecular formula,  $C_{33}H_{35}ClO_{11}$  (16 degrees of unsaturation), as **4** by HRESIMS analysis. Interpretation of its  $^1H$  and  $^{13}C$  NMR data (Table 3) and  $^1H$ – $^1H$  COSY and HMBC correlations indicated that it is a stereoisomer of **4**. The C-5/C-13 olefin in **5** was assigned the *E* geometry by NOESY correlations of H-9 with H-14b and of H-4 with H-18 (Figure 2). The epoxycyclohexanediol unit was similarly proposed to have the same absolute configuration as in **1**–**4** on the basis of  $^1H$ – $^1H$  coupling constants, NOESY correlations (Figure 2), and biosynthetic considerations, while the absolute configuration for C-1, C-9, and C-10 was deduced by comparison of the experimental and simulated ECD spectra generated by TDDFT using the same simplified structure **8** (Figure 3). The absolute configuration of **5** was then extrapolated by comparison of the experimental and calculated ECD spectra of **8a**–**d**. The experimental CD spectrum of **5** is comparable only to the calculated ECD curve of **8c** (Figure 4), correlating to the 1*R*,9*R*,10*R*,15*S*,16*S*,17*R*,18*R* absolute configuration.

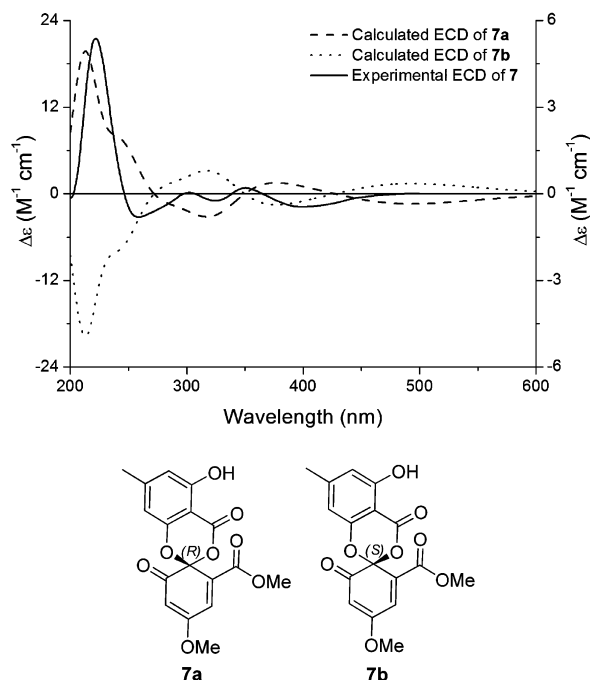


**Figure 4.** Experimental CD spectrum of **5** in MeOH and the calculated ECD spectra of **8a**–**d**.

Chloropestolide G (**6**) was assigned the molecular formula  $C_{32}H_{31}ClO_{10}$  (17 degrees of unsaturation) by HRESIMS, which is 32 mass units less than that of **4**. Analysis of its  $^1H$  and  $^{13}C$  NMR data (Table 3) revealed structural features similar to those found in **4**, except for the epoxycyclohexane-1,4-diol moiety. Specifically, the resonances for OH-18 and the C-25 methoxy were not observed in the spectra of **6**; the resonances for the C-5  $sp^2$  quaternary carbon and C-14 methylene unit in **4** were replaced by those for a methine ( $\delta_H/\delta_C$  3.56/34.0) and a  $sp^2$  carbon bearing a hydrogen ( $\delta_H/\delta_C$  5.64/126.8), respectively. These observations were supported by relevant  $^1H$ – $^1H$  COSY and HMBC correlations. HMBC cross peaks from H-4 and H-9 to C-13 and from H-14 to C-5 connected the isoprenylated 2,3-epoxycyclohexenol to the chlorinated tetrahydronaphthalen-2(1*H*)-one via the C-5–C-13 linkage. Considering the downfield chemical shifts for the C-18 oxymethine ( $\delta_H$  5.35 in **6** vs 4.82 in **4**;  $\delta_C$  76.9 in **6** vs 65.8 in **4**), together with the unsaturation requirement for **6**, both C-8 and C-18 were attached to the remaining oxygen atom to form a pyran ring, thereby completing the gross structure of **6**. Analysis of the NOESY data of **6** (Figure 2) revealed the same relative configuration as **4**, except for the C-5 stereogenic center, which was defined by a NOESY correlation of H-5 with H-18.

Therefore, the absolute configuration of **6** was proposed to be 1*S*,5*S*,9*S*,10*R*,15*S*,16*S*,17*R*,18*R*.

The molecular formula of **7** was determined to be  $C_{17}H_{14}O_8$  (11 degrees of unsaturation) by HRESIMS. A literature search on this formula readily identified dechloromaldoxin,<sup>18</sup> a synthetic racemate possessing the same planar structure as **7**, which was confirmed by interpretation of the 2D NMR data. The absolute configuration of **7** was proposed by comparison of the experimental and calculated ECD spectra generated for enantiomers (2*R*)-**7** (**7a**) and (2*S*)-**7** (**7b**) (Figure 5). An

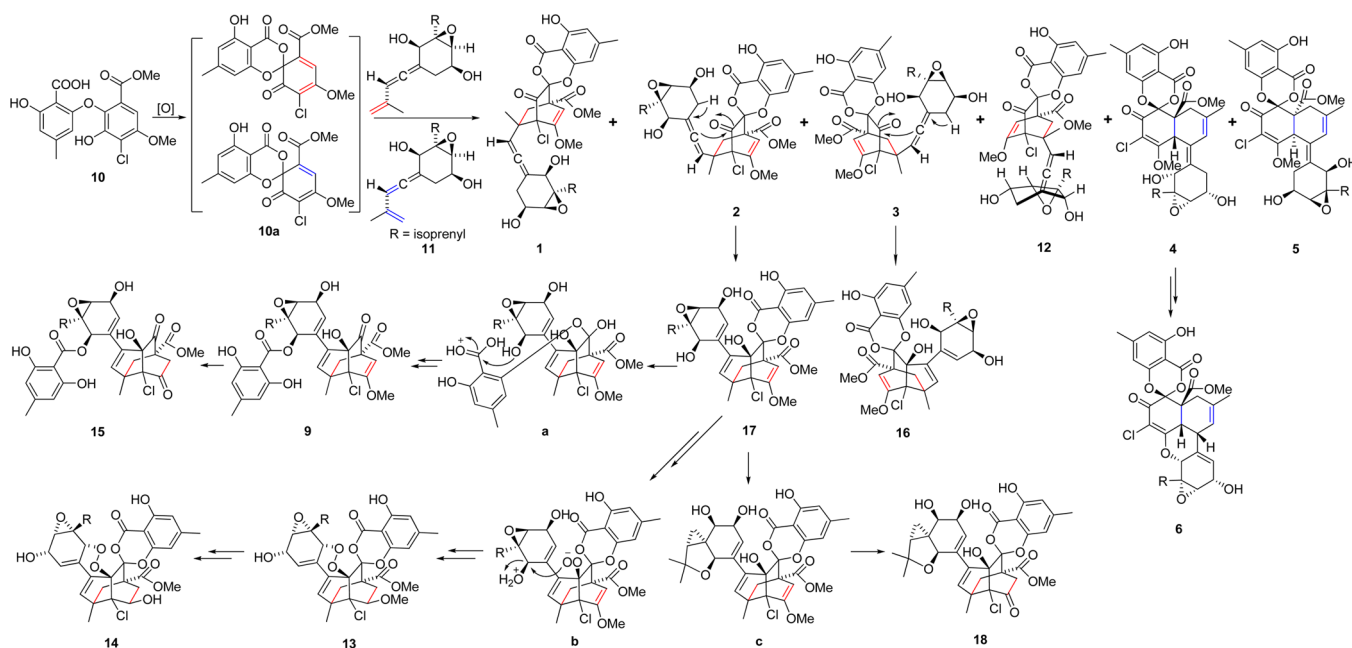


**Figure 5.** Experimental CD spectrum of **7** in MeOH and the calculated ECD spectra of two enantiomers, (2*R*)-**7** (**7a**) and (2*S*)-**7** (**7b**).

MMFF94 conformational search followed by B3LYP/6-31G(d) DFT reoptimization afforded four lowest-energy conformers (Figure S22 (Supporting Information)). The calculated ECD spectra of **7a,b** were then generated by Boltzmann weighting of their lowest-energy conformers (Figure 5). The experimental CD spectrum of **7** matches the calculated ECD curve of **7a** but is opposite to that of **7b**, suggesting the 2*R* configuration. To our knowledge, this is the first demonstration of the natural occurrence of optically pure dechloromaldoxin.

Compounds **1**–**7** were tested for cytotoxicity against three human tumor cell lines: CNE1-LMP1 (stable oncoprotein LMP1 integrated nasopharyngeal carcinoma cells), A375 (malignant melanoma cells), and MCF-7 (breast cancer cells). Compound **1** was cytotoxic to the three cell lines, showing  $IC_{50}$  values of 16.4, 9.9, and 23.6  $\mu M$ , respectively, while the positive control paclitaxel showed  $IC_{50}$  values of 4.2, 8.9, and 0.14 nM, respectively. The other compounds did not show detectable cytotoxicity against the three cell lines at 20  $\mu g/mL$ .

Natural products possessing the bicyclo[2.2.2]oct-2-en-5-one unit were mainly isolated from plants.<sup>23</sup> In addition, some synthetic compounds with the chlorinated bicyclo[2.2.2]oct-2-en-5-one core have been reported.<sup>24</sup> Prior to the discovery of chloropestolide A (**12**),<sup>11</sup> the only fungal metabolite incorpo-

Scheme 1. Plausible Biosynthetic Pathways for 1–6 and Previously Isolated 9<sup>7</sup> and 12–18<sup>11–13</sup>

rating the bicyclo[2.2.2]oct-2-en-5-one moiety was sorbiquinol, a polyketide isolated from *Trichoderma longibrachiatum*.<sup>25</sup> Structurally, chloropetstolides B–D (1–3) are stereoisomers of the previously isolated 12, all possessing the unique chlorinated spiro[benzo[*d*][1,3]dioxine-2,7'-bicyclo[2.2.2]octane]-4,8'-dione core, in which the bicyclo[2.2.2]oct-2-en-5-one is spirally joined to the benzo[*d*][1,3]dioxin-4-one unit at C-10 and connected to the isoprenylated epoxyvinylidenecyclohexanediol unit at C-3, while the benzo[*d*][1,3]dioxin-4-one unit is spirally joined to the 4a,5,8,8a-tetrahydronaphthalen-2(1*H*)-one moiety at C-10 to form the spiro[benzo[*d*][1,3]dioxine-2,1'-naphthalene]-2',4-dione skeleton found in 4–6.

Biogenetically, the coisolated pestheic acid (10) and iso-A82775C (11)<sup>7</sup> are the Diels–Alder precursors, not only for 9 and 12–18 but also for 1–6 (Scheme 1). Compound 10 is first oxidized to maldoxin (10a), which reacts with 11 via the REDDA and NEDDA routes to form the core structures of these metabolites. The REDDA reaction with 10a as a diene and 11 as a dienophile afforded adducts 1–3 and 12. Specifically, the *endo* and *exo* additions from the carboxylate face of 10a with 11 afford 1 and 2, respectively, whereas the *exo* and *endo* additions from the ether face of 10a with 11 provided 3 and 12, respectively. Compounds 4–6 are the NEDDA adducts, in which 10a reacted as a dienophile and 11 as a diene. The ratio for the six isolated Diels–Alder adducts (1–5 and 12) from 10a and 11 was 19:10:1:5:1:3, suggesting that the REDDA products generated from the reaction at the carboxylate face of 10a are the major ones. Therefore, the facial selectivity for the naturally occurring REDDA reaction is consistent with that found in laboratory synthesis.<sup>19</sup> The results were also supported by the crystal structure of dechloromaldoxin (7), in which the pseudoequatorially oriented carboxylate could make the diene in 10a more accessible for additions.<sup>18,19</sup> Since maldoxin (10a) was proved to be more reactive than its dechloro congener 7, which reacted only as a dienophile,<sup>19</sup> 10a was not isolated from *P. fici* possibly owing to its high reactivity with 11. The discovery of these unique spiroketals from *P. fici* not only provided evidence for the previously proposed

biogenesis of 16 and 17<sup>13</sup> by identifying their key intermediates 3 and 2 but also revealed the existence of naturally diversified Diels–Alder reaction cascades in the fungus.

## EXPERIMENTAL SECTION

**General Experimental Procedures.** Optical rotations were recorded using a 1 dm cell in CH<sub>3</sub>OH solvent. UV and CD spectra were run as methanol solutions. NMR spectra were recorded at either 500 or 600 MHz for <sup>1</sup>H nuclei and 125 or 150 MHz for <sup>13</sup>C nuclei. Residual solvent signals were used as reference (acetone-*d*<sub>6</sub>: δ<sub>H</sub> 2.05; δ<sub>C</sub> 29.8, 206.1). The HMQC and HMBC experiments were optimized for 145.0 and 8.0 Hz, respectively. ESIMS data and HRESIMS data were obtained using a Q-TOF LC/MS instrument equipped with an electrospray ionization (ESI) source. The fragmentor and capillary voltages were kept at 125 and 3500 V, respectively. Nitrogen was supplied as the nebulizing and drying gas. The temperature of the drying gas was set at 300 °C. The flow rate of the drying gas and the pressure of the nebulizer were 10 L/min and 10 psi, respectively. All MS experiments were performed in positive ion mode. Full-scan spectra were acquired over a scan range of *m/z* 100–1000 at 1.03 spectra/s.

**Fungal Material.** The culture of *P. fici* was isolated from the branches of *Camellia sinensis* (Theaceae) in a suburb of Hangzhou, People's Republic of China, in April 2005. The isolate was identified as *P. fici* by one of the authors (L.G.) on the basis of sequence (GenBank accession number DQ812914) analysis of the ITS region of the rDNA and assigned the accession number AS 3.9138 in the China General Microbial Culture Collection (CGMCC) at the Institute of Microbiology, Chinese Academy of Sciences, Beijing. The fungal strain was cultured on slants of potato dextrose agar (PDA) at 25 °C for 10 days. Agar plugs were cut into small pieces (about 0.5 × 0.5 × 0.5 cm<sup>3</sup>) under aseptic conditions, and 15 pieces were used to inoculate three Erlenmeyer flasks (250 mL), each containing 50 mL of media (0.4% glucose, 1% malt extract, and 0.4% yeast extract; the final pH of the media was adjusted to 6.5 and sterilized by autoclave). Three flasks of the inoculated media were incubated at 25 °C on a rotary shaker at 170 rpm for 5 days to prepare the seed culture. Spore inoculum was prepared by suspension in sterile, distilled H<sub>2</sub>O to give a final spore/cell suspension of 1 × 10<sup>6</sup>/mL. Fermentation was carried out in 36 Fernbach flasks (500 mL), each containing 80 g of rice. Distilled H<sub>2</sub>O (120 mL) was added to each flask, and the contents were soaked overnight before autoclaving at 15 psi for 30 min. After they were



cooled to room temperature, each flask was inoculated with 5.0 mL of the spore inoculum and incubated at 25 °C for 40 days.

**Extraction and Isolation.** The fermented material was extracted repeatedly with EtOAc (4 × 3.0 L), and the organic solvent was evaporated to dryness under vacuum to afford the crude extract (33 g), which was fractionated by silica gel VLC using petroleum ether–EtOAc gradient elution. The fraction (520 mg) with the unidentified components was eluted with 36% EtOAc and further separated by Sephadex LH-20 column chromatography (CC) with 1/1 CH<sub>2</sub>Cl<sub>2</sub>/MeOH as eluent. The resulting subfractions were purified by semipreparative RP HPLC (C<sub>18</sub> column; 5 μm; 9.4 × 250 mm; 70% MeOH in H<sub>2</sub>O for 2 min, followed by 70–80% over 48 min; 2 mL/min) to afford **1** (57.3 mg, *t<sub>R</sub>* = 42.70 min), **4** (15.1 mg, *t<sub>R</sub>* = 33.50 min), and **5** (3.2 mg, *t<sub>R</sub>* = 46.10 min). The fractions eluted with 30% (160 mg), 32% (280 mg), and 34% EtOAc (270 mg) were individually separated by Sephadex LH-20 CC with 1/1 CH<sub>2</sub>Cl<sub>2</sub>/MeOH as eluent. Purification of the resulting subfractions by RP HPLC (C<sub>18</sub> column; 5 μm; 9.4 × 250 mm) afforded the mixtures of **2** and **17** (30.1 mg, 25:1, *t<sub>R</sub>* = 27.80 min; 65% MeOH in H<sub>2</sub>O for 2 min, followed by 65–80% over 40 min; 2 mL/min), **3** and **16** (3.3 mg, 9:1, *t<sub>R</sub>* = 40.80 min; 62% MeOH in H<sub>2</sub>O for 2 min, followed by 62–75% over 45 min; 2 mL/min), and pure **6** (2.5 mg, *t<sub>R</sub>* = 21.80 min; 70% MeOH in H<sub>2</sub>O for 2 min, followed by 70–83% over 25 min; 2 mL/min) and **7** (2.0 mg, *t<sub>R</sub>* = 15.5 min; 65% MeOH in H<sub>2</sub>O for 2 min, followed by 65–80% over 25 min; 2 mL/min).

**Chloropestolide B (1):** yellow oil; [ $\alpha$ ]<sub>D</sub><sup>25</sup> = −35° (c 0.10, MeOH); UV (MeOH)  $\lambda_{\text{max}}$  (log  $\epsilon$ ) 222 (4.24), 264 (3.99) nm; IR (neat)  $\nu_{\text{max}}$  3436 (br), 2970, 1709, 1739, 1709, 1641, 1464, 1360, 1203, 1039 cm<sup>−1</sup>; for <sup>1</sup>H, <sup>13</sup>C NMR, HMBC, and NOESY data see Table 1; HRESIMS *m/z* 665.1765 (calcd for C<sub>33</sub>H<sub>35</sub>ClO<sub>11</sub>Na, 665.1760).

**Chloropestolide C (2):** pale yellow oil; [ $\alpha$ ]<sub>D</sub><sup>25</sup> = +25° (c 0.10, MeOH); UV (MeOH)  $\lambda_{\text{max}}$  (log  $\epsilon$ ) 227 (4.14), 255 (3.78) nm; IR (neat)  $\nu_{\text{max}}$  3447 (br), 2957, 1739, 1739, 1694, 1465, 1366, 1205, 1022 cm<sup>−1</sup>; for <sup>1</sup>H, <sup>13</sup>C NMR, and HMBC data see Table 2. NOESY correlations (acetone-*d*<sub>6</sub>, 500 MHz): H-2a ↔ H-9, H-12; H-2b ↔ H-4; H-4 ↔ H-2b, H<sub>3</sub>-12; H-9 ↔ H-2a; H<sub>3</sub>-12 ↔ H-2a, H-4; H-16 ↔ H<sub>2</sub>-19, H-20; H-18 ↔ H<sub>2</sub>-19, H-20; H<sub>2</sub>-19 ↔ H-16, H-18; H-20 ↔ H-16, H-18. HRESIMS: *m/z* 665.1770 (calcd for C<sub>33</sub>H<sub>35</sub>ClO<sub>11</sub>Na, 665.1760).

**Chloropestolide D (3):** pale yellow oil; [ $\alpha$ ]<sub>D</sub><sup>25</sup> = +8.0° (c 0.10, MeOH); UV (MeOH)  $\lambda_{\text{max}}$  (log  $\epsilon$ ) 227 (4.05), 255 (3.50) nm; IR (neat)  $\nu_{\text{max}}$  3410 (br), 2928, 1972, 1739, 1708, 1694, 1454, 1360, 1204, 1035 cm<sup>−1</sup>; for <sup>1</sup>H, <sup>13</sup>C NMR, and HMBC data see Table 2. NOESY correlations (acetone-*d*<sub>6</sub>, 600 MHz): H-2a ↔ H-9, H-12; H-2b ↔ H-4; H-4 ↔ H-2b, H<sub>3</sub>-12; H-9 ↔ H-2a; H<sub>3</sub>-12 ↔ H-2a, H-4; H-16 ↔ H<sub>2</sub>-19; H-18 ↔ H<sub>2</sub>-19; H<sub>2</sub>-19 ↔ H-16, H-18. HRESIMS: *m/z* 643.1937 (calcd for C<sub>33</sub>H<sub>36</sub>ClO<sub>11</sub>, 643.1941).

**Chloropestolide E (4):** pale yellow oil; [ $\alpha$ ]<sub>D</sub><sup>25</sup> = −468° (c 0.10, MeOH); UV (MeOH)  $\lambda_{\text{max}}$  (log  $\epsilon$ ) 251 (4.00), 218 (4.02) nm; CD (c 1.0 × 10<sup>−3</sup> M, MeOH)  $\lambda_{\text{max}}$  ( $\Delta\epsilon$ ) 218 (+23.16), 273 (−18.10), 343 (−5.71) nm; IR (neat)  $\nu_{\text{max}}$  3400 (br), 2925, 1710, 1640, 1576, 1438, 1360, 1199, 1028 cm<sup>−1</sup>; for <sup>1</sup>H, <sup>13</sup>C NMR, and HMBC data see Table 3. NOESY correlations (acetone-*d*<sub>6</sub>, 600 MHz): H-4 ↔ H-14b; H-9 ↔ H-18; H-14b ↔ H-4; H-16 ↔ H-19a, H-20; H-18 ↔ H-9, H-20; H-19a ↔ H-16; H-20 ↔ H-16, H-18. HRESIMS: *m/z* 643.1946 (calcd for C<sub>33</sub>H<sub>36</sub>ClO<sub>11</sub>, 643.1941).

**Chloropestolide F (5):** pale yellow oil; [ $\alpha$ ]<sub>D</sub><sup>25</sup> = −180° (c 0.10, MeOH); UV (MeOH)  $\lambda_{\text{max}}$  (log  $\epsilon$ ) 251 (4.12), 220 (4.15) nm; CD (c 1.0 × 10<sup>−3</sup> M, MeOH)  $\lambda_{\text{max}}$  ( $\Delta\epsilon$ ) 222 (+7.88), 247 (+6.03), 280 (−0.59), 314 (+2.37), 350 (−0.98) nm; IR (neat)  $\nu_{\text{max}}$  3385 (br), 2925, 1698, 1640, 1573, 1438, 1358, 1198, 1023 cm<sup>−1</sup>; for <sup>1</sup>H and <sup>13</sup>C NMR data see Table 3. HMBC data (acetone-*d*<sub>6</sub>, 600 MHz): H<sub>2</sub>-2 → C-1,3,4,9,10,11,12; H-4 → C-2,5,9,12; H-9 → C-1,2,4,5,7,8,11,13; H<sub>3</sub>-12 → C-2,3,4; H<sub>2</sub>-14 → C-5,13,15,16,18; H-16 → C-14,15,17,18; H-18 → C-14; H<sub>2</sub>-19 → C-16,17,20,21; H-20 → C-22,23; H<sub>3</sub>-22 → C-20,21,23; H<sub>3</sub>-23 → C-20,21,22; H<sub>3</sub>-24 → C-11; H<sub>3</sub>-25 → C-8; H-29 → C-27,28,31,33; H-31 → C-27,29,32,33; H<sub>3</sub>-33 → C-29,30,31; OH-28 → C-27,28,29. NOESY correlations (acetone-*d*<sub>6</sub>, 600 MHz): H-4 ↔ H-18; H-9 ↔ H-14b; H-14b ↔ H-9; H-18 ↔ H-4, H-19b; H-19b

↔ H-18. HRESIMS: *m/z* 665.1761 (calcd for C<sub>33</sub>H<sub>35</sub>ClO<sub>11</sub>Na, 665.1760).

**Chloropestolide G (6):** pale yellow oil; [ $\alpha$ ]<sub>D</sub><sup>25</sup> = +80° (c 0.10, MeOH); UV (MeOH)  $\lambda_{\text{max}}$  (log  $\epsilon$ ) 271 (4.13), 219 (4.08) nm; IR (neat)  $\nu_{\text{max}}$  3286 (br), 2925, 1709, 1640, 1581, 1438, 1358, 1012 cm<sup>−1</sup>; for <sup>1</sup>H and <sup>13</sup>C NMR data see Table 3. HMBC data (acetone-*d*<sub>6</sub>, 600 MHz): H<sub>2</sub>-2 → C-1,3,4,9,10,11,12; H-4 → C-2,3,5,9,12,13; H-9 → C-1,2,4,5,6,7,8,10,11,13; H<sub>3</sub>-12 → C-2,3,4; H-14 → C-5,16,18; H-16 → C-14,15,17,19; H-18 → C-5,13,14,19; H<sub>2</sub>-19 → C-16,17,18,20,21; H-20 → C-19,22,23; H<sub>3</sub>-22 → C-20,21,23; H<sub>3</sub>-23 → C-20,21,22; H<sub>3</sub>-24 → C-11; H-29 → C-26,27,28,31,33; H-31 → C-26,27,29,32,33; H<sub>3</sub>-33 → C-29,30,31; NOESY correlations (acetone-*d*<sub>6</sub>, 500 MHz) H-4 ↔ H-14; H-5 ↔ H-18; H-9 ↔ H-18; H-14 ↔ H-4; H-16 ↔ H-19a, H-20; H-18 ↔ H-5, H-9; H-19a ↔ H-16; H-20 ↔ H-16; HRESIMS *m/z*: 633.1496 (calcd for C<sub>32</sub>H<sub>31</sub>ClO<sub>10</sub>Na, 633.1498).

**Dechloromaldoxin (7):** yellow powder; [ $\alpha$ ]<sub>D</sub><sup>25</sup> = −30° (c 0.10, MeOH); UV (MeOH)  $\lambda_{\text{max}}$  (log  $\epsilon$ ) 225 (3.95) nm; CD (c 4.8 × 10<sup>−3</sup> M, MeOH)  $\lambda_{\text{max}}$  ( $\Delta\epsilon$ ) 222 (+5.36), 247 (+6.03), 260 (−0.80), 400 (−0.45) nm; IR (neat)  $\nu_{\text{max}}$  3248 (br), 2928, 1729, 1709, 1673, 1639, 1593, 1463, 1383, 1201, 1012 cm<sup>−1</sup>; <sup>1</sup>H NMR (acetone-*d*<sub>6</sub>, 500 MHz)  $\delta$  9.99 (1H, s, OH-5), 7.27 (1H, d, *J* = 2.0 Hz, H-2'), 6.48 (1H, s, H-6), 6.26 (1H, s, H-8), 5.73 (1H, d, *J* = 2.0 Hz, H-4'), 4.00 (3H, s, H<sub>3</sub>-8'), 3.82 (3H, s, H<sub>3</sub>-7'), 2.28 (3H, s, H<sub>3</sub>-11); <sup>13</sup>C NMR (acetone-*d*<sub>6</sub>, 125 MHz)  $\delta$  188.9 (C, C-5'), 168.9 (C, C-3'), 164.2 (C, C-4), 162.3 (C, C-6'), 161.2 (C, C-5), 154.7 (C, C-9), 151.1 (C, C-7), 136.4 (CH, C-2'), 134.5 (C, C-1'), 112.2 (CH, C-6), 108.0 (CH, C-8), 99.6 (CH, C-4'), 97.4 (C, C-10), 93.7 (C, C-2), 58.2 (CH<sub>3</sub>, C-8'), 53.0 (CH<sub>3</sub>, C-7'), 22.3 (CH<sub>3</sub>, C-11). HMBC data (acetone-*d*<sub>6</sub>, 600 MHz): H-6 → C-5,8,10,11; H-8 → C-6,9,10,11; H<sub>3</sub>-11 → C-6,7,8; H-2' → C-2,4',6'; H-4' → C-2,2'; H<sub>3</sub>-7' → C-6'; H<sub>3</sub>-8' → C-3'; OH-5 → C-5,6,10. HRESIMS: *m/z* 347.0760 (calcd for C<sub>17</sub>H<sub>15</sub>O<sub>8</sub>, 347.0761).

**Computational Details.** Systematic conformational analyses for **4**, **5**, and **7** were performed via the molecular operating environment (MOE) version 2009.10 (Chemical Computing Group, Canada) software package using the MMFF94 molecular mechanics force field calculation. The MMFF94 conformational analyses were further optimized using TDDFT at the B3LYP/6-31G(d) basis set level. The stationary points have been checked as the true minima of the potential energy surface by verifying that they do not exhibit vibrational imaginary frequencies. The 30 lowest electronic transitions were calculated, and the rotational strengths of each electronic excitation were given using both dipole length and dipole velocity representations. ECD spectra were stimulated using a Gaussian function with a half-bandwidth of 0.3 eV. Equilibrium populations of conformers at 298.15 K were calculated from their relative free energies ( $\Delta G$ ) using Boltzmann statistics. The overall ECD spectra were then generated according to Boltzmann weighting of each conformer. The systematic errors in the prediction of the wavelength and excited-state energies are compensated for by employing UV correlation. All quantum computations were performed using the Gaussian03 package,<sup>26</sup> on an IBM cluster machine located at the High Performance Computing Center of Peking Union Medical College.

**MTS Assay.**<sup>27</sup> The assay was run in triplicate. In a 96-well plate, each well was plated with (2–5) × 10<sup>3</sup> cells (depending on the cell multiplication rate). After cell attachment overnight, the medium was removed, and each well was treated with 100 μL of medium containing 0.1% DMSO or appropriate concentrations of the test compounds and the positive control paclitaxel (Sigma) (100 mM as a stock solution of the compound in DMSO and serial dilutions; the test compounds showed good solubility in DMSO and did not precipitate when added to the cells). The plate was incubated for 48 h at 37 °C in a humidified, 5% CO<sub>2</sub> atmosphere. Proliferation was assessed by adding 20 μL of MTS (Promega) to each well in the dark, followed by a 90 min incubation at 37 °C. The assay plate was read at 490 nm using a microplate reader.



## ■ ASSOCIATED CONTENT

## ■ Supporting Information

Figures giving  $^1\text{H}$  and  $^{13}\text{C}$  NMR spectra of 1–7 and UV and CD calculations for 4, 5, and 7. This material is available free of charge via the Internet at <http://pubs.acs.org>.

## ■ AUTHOR INFORMATION

## Corresponding Author

\*Tel/Fax: +86 10 66932679. E-mail: cheys@im.ac.cn (Y.Che); ycao98@vip.sina.com (Y.Cao).

## Notes

The authors declare no competing financial interest.

## ■ ACKNOWLEDGMENTS

We gratefully acknowledge financial support from the National Natural Science Foundation of China (30925039 and 21002120), the Beijing Natural Science Foundation (5111003), the Ministry of Science and Technology of China (2012ZX09301-003 and 2012AA021703), and the Chinese Academy of Sciences (KSCX2-EW-G-6).

## ■ REFERENCES

- (1) Aly, A. H.; Debbab, A.; Kjer, J.; Proksch, P. *Fungal Divers.* **2010**, *41*, 1–6.
- (2) Schulz, B.; Boyle, C.; Draeger, S.; Rommert, A. K.; Krohn, K. *Mycol. Res.* **2002**, *106*, 996–1004.
- (3) Strobel, G. A. *Microbes Infect.* **2003**, *5*, 535–544.
- (4) Tan, R. X.; Zou, W. X. *Nat. Prod. Rep.* **2001**, *18*, 448–459.
- (5) (a) Wang, L. W.; Zhang, Y. L.; Lin, F. C.; Hu, Y. Z.; Zhang, C. L. *Mini-Rev. Med. Chem.* **2011**, *11*, 1056–1074. (b) Yang, X. L.; Zhang, J. Z.; Luo, D. Q. *Nat. Prod. Rep.* **2012**, *29*, 622–641.
- (6) (a) Ding, G.; Liu, S.; Guo, L.; Zhou, Y.; Che, Y. *J. Nat. Prod.* **2008**, *71*, 615–618. (b) Li, E.; Tian, R.; Liu, S.; Chen, X.; Guo, L.; Che, Y. *J. Nat. Prod.* **2008**, *71*, 664–668. (c) Li, E.; Jiang, L.; Guo, L.; Zhang, H.; Che, Y. *Bioorg. Med. Chem.* **2008**, *16*, 7894–7899. (d) Ding, G.; Zheng, Z.; Liu, S.; Zhang, H.; Guo, L.; Che, Y. *J. Nat. Prod.* **2009**, *72*, 942–945. (e) Li, J.; Li, L.; Si, Y.; Jiang, X.; Guo, L.; Che, Y. *Org. Lett.* **2011**, *13*, 2670–2673.
- (7) Liu, L.; Liu, S.; Jiang, L.; Chen, X.; Guo, L.; Che, Y. *Org. Lett.* **2008**, *10*, 1397–1400.
- (8) Liu, L.; Tian, R.; Liu, S.; Chen, X.; Guo, L.; Che, Y. *Bioorg. Med. Chem.* **2008**, *16*, 6021–6026.
- (9) Liu, L.; Liu, S.; Chen, X.; Guo, L.; Che, Y. *Bioorg. Med. Chem.* **2009**, *17*, 606–613.
- (10) Liu, L.; Liu, S.; Niu, S.; Guo, L.; Chen, X.; Che, Y. *J. Nat. Prod.* **2009**, *72*, 1482–1486.
- (11) Liu, L.; Li, Y.; Liu, S.; Zheng, Z.; Chen, X.; Guo, L.; Che, Y. *Org. Lett.* **2009**, *11*, 2836–2839.
- (12) Liu, L.; Niu, S.; Lu, X.; Chen, X.; Zhang, H.; Guo, L.; Che, Y. *Chem. Commun.* **2010**, *46*, 460–462.
- (13) Liu, L.; Bruhn, T.; Guo, L.; Götz, D. C. G.; Brun, B.; Stich, A.; Che, Y.; Bringmann, G. *Chem. Eur. J.* **2011**, *17*, 2604–2613.
- (14) Adeboya, M. O.; Edwards, R. L.; Lassøe, T.; Maitland, D. J.; Shields, L.; Whalley, A. J. *J. Chem. Soc., Perkin Trans. 1* **1996**, 1419–1425.
- (15) (a) Liao, C. C.; Peddinti, P. K. *Acc. Chem. Res.* **2002**, *35*, 856–866. (b) Liao, C. C. *Pure Appl. Chem.* **2005**, *77*, 1221–1234.
- (16) Ayadi, S.; Abderrabba, M. *Russ. J. Phys. Chem. A* **2008**, *82*, 1080–1085.
- (17) Suzuki, T.; Kobayashi, S. *Org. Lett.* **2010**, *12*, 2920–2932.
- (18) Yu, M.; Snider, B. B. *Org. Lett.* **2011**, *13*, 4224–4227.
- (19) Yu, M.; Snider, B. B. *Tetrahedron* **2011**, *67*, 9473–9478.
- (20) Huang, X.; He, J.; Niu, X.; Menzel, K.; Dahse, H.; Grabley, S.; Fiedler, H.; Sattler, I.; Hertweck, C. *Angew. Chem., Int. Ed.* **2008**, *47*, 3995–3998.
- (21) (a) Diedrich, C.; Grimme, S. *J. Phys. Chem. A* **2003**, *107*, 2524–2539. (b) Crawford, T. D.; Tam, M. C.; Abrams, M. L. *J. Phys. Chem. A* **2007**, *111*, 12058–12068. (c) Stephens, P. J.; Devlin, F. J.; Gasparini, F.; Ciogli, A.; Spinelli, D.; Cosimelli, B. *J. Org. Chem.* **2007**, *72*, 4707–4715. (d) Ding, Y.; Li, X. C.; Ferreira, D. *J. Org. Chem.* **2007**, *72*, 9010–9017. (e) Berova, N.; Bari, L. D.; Pescitelli, G. *Chem. Soc. Rev.* **2007**, *36*, 914–931. (f) Bringmann, G.; Bruhn, T.; Maksimenka, K.; Hemberger, Y. *Eur. J. Org. Chem.* **2009**, 2717–2727.
- (22) Xing, Q.; Pei, W.; Xu, R.; Pei, J. *Basic Organic Chemistry*, 3rd ed.; High Education Press: Beijing, 2005; pp 346–347.
- (23) (a) Yamamura, S.; Niwa, M.; Nonoyama, M.; Terada, Y. *Tetrahedron Lett.* **1978**, *19*, 4891–4894. (b) Escher, S.; Keller, U.; Willhalm, B. *Helv. Chim. Acta* **1979**, *62*, 2061–2072. (c) Lins, A. P.; Ribeiro, M. N.; Gottlieb, O. R.; Gottlieb, H. E. *J. Nat. Prod.* **1982**, *45*, 754–761. (d) Tanaka, T.; Nishimura, I. K.; Nonaka, G.; Young, T. J. *Nat. Prod.* **1996**, *59*, 843–849. (e) Kuo, Y. H.; Chen, C. H.; Huang, S. L. *Chem. Pharm. Bull.* **1998**, *46*, 181–183. (f) Tezuka, Y.; Terazono, M.; Kusumoto, T. I.; Kawashima, Y.; Hatanaka, Y.; Kadota, S.; Hattori, M.; Namba, T.; Kikuchi, T. *Helv. Chim. Acta* **1999**, *82*, 408–417. (g) Su, B. N.; Zhu, Q. X.; Jia, Z. J. *Tetrahedron Lett.* **1999**, *40*, 357–358. (h) Chien, S. C.; Chang, J. Y.; Kuo, C. C.; Hsieh, C. C.; Yang, N. S.; Kuo, Y. H. *Tetrahedron Lett.* **2007**, *48*, 1567–1569.
- (24) (a) Ansell, M. F.; Leslie, V. J. *Chem. Commun.* **1967**, *18*, 949–950. (b) Ansell, M. F.; Leslie, V. J. *J. Chem. Soc. C* **1971**, *8*, 1423–1429.
- (25) Romano, A.; William, A. A.; Latchezar, S. T. *Can. J. Chem.* **1996**, *74*, 371–379.
- (26) Frisch, M. J.; Trucks, G. W.; Schlegel, H. B.; Scuseria, G. E.; Robb, M. A.; Cheeseman, J. R.; Montgomery, J. A., Jr.; Vreven, T.; Kudin, K. N.; Burant, J. C.; Millam, J. M.; Iyengar, S. S.; Tomasi, J.; Barone, V.; Mennucci, B.; Cossi, M.; Scalmani, G.; Rega, N.; Petersson, G. A.; Nakatsuji, H.; Hada, M.; Ehara, M.; Toyota, K.; Fukuda, R.; Hasegawa, J.; Ishida, M.; Nakajima, T.; Honda, Y.; Kitao, O.; Nakai, H.; Klene, M.; Li, X.; Knox, J. E.; Hratchian, H. P.; Cross, J. B.; Bakken, V.; Adamo, C.; Jaramillo, J.; Gomperts, R.; Stratmann, R. E.; Yazyev, O.; Austin, A. J.; Cammi, R.; Pomelli, C.; Ochterski, J. W.; Ayala, P. Y.; Morokuma, K.; Voth, G. A.; Salvador, P.; Dannenberg, J. J.; Zakrzewski, V. G.; Dapprich, S.; Daniels, A. D.; Strain, M. C.; Farkas, O.; Malick, D. K.; Rabuck, A. D.; Raghavachari, K.; Foresman, J. B.; Ortiz, J. V.; Cui, Q.; Baboul, A. G.; Clifford, S.; Cioslowski, J.; Stefanov, B. B.; Liu, G.; Liashenko, A.; Piskorz, P.; Komaromi, I.; Martin, R. L.; Fox, D. J.; Keith, T.; Al-Laham, M. A.; Peng, C. Y.; Nanayakkara, A.; Challacombe, M.; Gill, P. M. W.; Johnson, B.; Chen, W.; Wong, M. W.; Gonzalez, C.; Pople, J. A. *Gaussian 03, Revision E.01*; Gaussian, Inc., Wallingford, CT, 2004.
- (27) Zhang, N.; Chen, Y.; Jiang, R.; Li, E.; Chen, X.; Xi, Z.; Guo, Y.; Liu, X.; Zhou, Y.; Che, Y.; Jiang, X. *Autophagy* **2011**, *7*, 598–612.